PRAMANA
— journal of
physics

Vol. 78, No. 5
May 2012
pp. 791–801

Crystal growth, FTIR and thermal characterization of bis(ethyltriphenylphosphonium) tetrabromomanganate(II) dihydrate crystals

C ILAMARAN, M SETHURAM, M DHANDAPANI* and G AMIRTHAGANESAN

Post Graduate and Research Department of Chemistry, Sri Ramakrishna Mission Vidyalaya College of Arts and Science, Coimbatore 641 020, India
*Corresponding author. E-mail: srmvdhandapani@gmail.com

MS received 13 March 2011; revised 26 December 2011; accepted 11 January 2012

Abstract. Single crystals of a novel compound, bis(ethyltriphenylphosphonium) tetrabromomanganate(II) dihydrate (BTP-Mn) were grown by solution growth-slow evaporation technique from aqueous solution of the compound at ambient temperature. The grown crystals were characterized by elemental analysis, powder X-ray diffraction, thermal analysis, nuclear magnetic resonance spectroscopy (NMR) and Fourier transform infra-red spectroscopy (FTIR) techniques. The chemical composition of the compound was revealed by elemental analysis and its crystallinity was confirmed by powder X-ray diffraction. Thermal analysis confirmed that the compound was stable up to 125°C. The various kinds of protons and carbons present in the compound were confirmed by ^{1}H NMR and ^{13}C NMR technique respectively and the presence of phosphorous was confirmed by ^{31}P NMR spectrum in the compound. The modes of vibration of different molecular groups present in the compound were identified by FTIR spectral analysis. The second harmonic generation behaviour was tested by Nd:YAG laser source.

Keywords. Inorganic compounds; X-ray diffraction; Fourier transform spectrum; differential thermal analysis; optical properties.

PACS Nos 61.66.Fn; 61.05.C−; 33.20.Ea; 81.70.Pg

1. Introduction

Bis(ethyltriphenylphosphonium) tetrabromomanganate(II) dihydrate crystals (BTP-Mn) belong to a family characterized by the general formula A_2BX_4. The prototype of the crystal structure of this family is β-K_2SO_4 which consists of isolated BX_4^{2-} tetrahedra and monovalent A^+ cations placed in two inequivalent cavities [1]. An essential feature of the members of the above group is that they undergo several phase transitions, both commensurate (C) and incommensurate (IC) [2–8]. In the normal phase, these crystals are

orthorhombic and pseudohexagonal identical with β-K_2SO_4-type structure [9]. In the incommensurate phase, modulated polarization turns up with a period irrational to the period of the crystal lattice and in the commensurate phase some of the A_2BX_4 crystals have ferroelectricity or ferroelasticity [10]. There is another group of A_2BX_4 halides having the monoclinic structure Sr_2GeS_4 at room temperature [11].

Quaternary ammonium and phosphonium salts are effective phase transfer catalysts (PTC) for nucleophilic fluorination reactions by potassium fluoride. Both ammonium and phosphonium fluorides formed during the reactions are extremely reactive, with fluorination following a stereospecific SN^2 mechanism [12]. Chiral quaternary ammonium and phosphonium fluorides have interesting properties as novel reagents for simple asymmetric nucleophilic fluorination reaction studies. Phosphonium compounds are more effective in these reactions than ammonium compounds. Phosphonium salts have potential applications in communication technologies as photoresist materials [13]. Quaternary phosphonium salts can be made into casts with commercially available polymeric suspension to form membranes for the mass transport of cations, anions and neutral species [14]. However, no attempt has been made so far to crystallize these compounds and check their suitability for industrial applications. This paper deals with the growth and characterization of bis(ethyltriphenylphosphonium) tetrabromomanganate(II) dihydrate (BTP-Mn).

2. Material synthesis

The compound BTP-Mn was synthesized by reacting ethyltriphenylphosphonium bromide and manganese(II) bromide in 2 : 1 molar ratio in aqueous medium. The two solutions were mixed thoroughly and stirred well using mechanical stirrer for 4 h to get a homogeneous solution. The resulting solution was filtered and the filtrate was kept in dust-free environment. The crude material was recrystallized several times to get ultrapure material. The reaction takes place as per the following equation:

$$2[(C_6H_5)_3P\text{–}C_2H_5)Br] + MnBr_2 + 2H_2O \longrightarrow [(C_6H_5)_3P\text{–}CH_2\text{–}CH_3]_2MnBr_4 \cdot 2H_2O$$

BTP–Mn

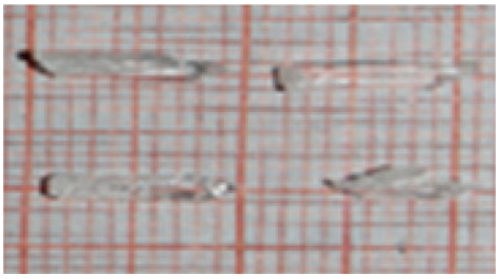

Figure 1. The photograph of the as-grown BTP-Mn crystal.

Bright, transparent and colourless crystals with average size of 8 × 2 × 2 mm were obtained within 15–20 days. Slow evaporation-solution growth technique was employed using triply distilled water as the medium at ambient temperature. The photograph of the as-grown crystals is shown in figure 1.

3. Characterization

The elemental analysis of the compound was carried out in an ELEMENTAR VARIO ELIII instrument. The powder X-ray diffraction of the crystals was carried out using Bruker AXS D8 diffractometer. The FTIR spectra of the compounds were obtained using Perkin Elmer model RX1 spectrometer employing KBr pellet technique. TG/DTA analyses were undertaken in a Perkin Elmer Diamond TG/DTA Thermal Analyser under nitrogen atmosphere at a heating rate of 10°C/min. The H^1, C^{13} and P^{31} NMR spectra of BTP-Mn were recorded in AVANCE III 500 MHz Bruker Facility using D_2O as the solvent.

4. Results and discussion

4.1 *Chemical structure*

The probable structure of the BTP-Mn compound is given in figure 2. The experimental results of various characterization measurements discussed in the following paragraphs led to this structure. However, single crystal X-ray diffraction data collection and refinement can only confirm the structure. The work is under progress and will be published elsewhere.

4.2 *Elemental analysis*

The elemental analysis shows that the compound contains carbon: 58.5% (57.90) and hydrogen: 4.0% (6.02). Theoretical values are given in brackets. The experimental and calculated values are very close to each other and are within the error limits. This confirms the formation of the compound in the proposed stoichiometric ratio.

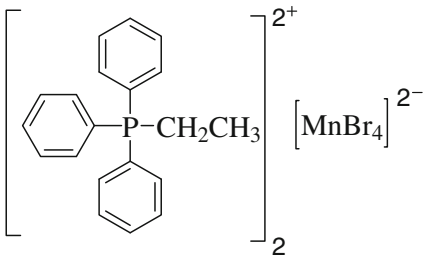

Figure 2. The probable structure of BTP-Mn.

4.3 *Powder X-ray diffraction*

The powder X-ray diffraction pattern of BTP-Mn is shown in figure 3. The sharp and well-defined Bragg peaks observed in the powder X-ray diffraction pattern confirm the crystalline nature of the compound. All the observed reflections were indexed. From the powder X-ray diffraction data the lattice parameters and the cell volume have been calculated. The unit cell parameters are: $a = 8.73702$ Å, $b = 12.98491$ Å, $c = 6.62657$ Å and $\alpha = \gamma = 90°$, $\beta = 95.7308°$. The unit cell volume is 748.02 Å^3. From the unit cell parameters, the title compound was found to crystallize in monoclinic crystal system. The observed $h\ k\ l$, 2θ and d values are given in table 1.

4.4 *Thermal analysis*

The TG and DTG curves of BTP-Mn are shown in figure 4. When the sample is heated from 40 to 800°C, a two-step decomposition pattern is observed. In the first step, two water molecules of crystallization from the compound get eliminated at 125°C. An experimental weight loss of 3.9% due to the elimination of two water molecules (equal to 36 molecular mass units) matches with the theoretical weight loss in the first step (3.5%). The second stage decomposition starts at 275°C and ends at 360°C. In this step, the anhydrous compound decomposes into smaller volatile fragments leaving no traceable residue as shown in figure 4. The total weight loss in the second stage is around 90.6% from a total of 100% taken initially. The weight loss is equal to 970 molecular units. This can be accounted for the loss of one mole of butane, two moles of triphenyl phosphonium bromide, and one molecule of bromine and Mn remain as a residue. The difference in the weight losses is due to the presence of adsorbed moisture in the crystal that is usually associated with hydrated crystals [15]. The decomposition pattern formulated is given below.

***Step* I**

$$\underset{\text{Formula weight: 1006}}{\left[C_2H_5\text{–}P\text{–}(C_6H_5)_3\right]_2[MnBr_4]\cdot 2H_2O} \xrightarrow{125-145^\circ C} \underset{\begin{array}{l}\text{Theoretical loss} \quad :3.5\% \\ \text{Experimental loss} \quad :3.9\%\end{array}}{\left[C_2H_5\text{–}P\text{–}(C_6H_5)_3\right]_2[MnBr_4] + 2H_2O\uparrow}$$

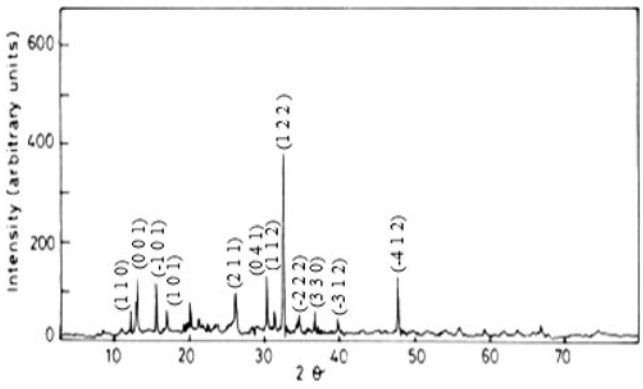

Figure 3. The powder X-ray diffraction pattern of BTP-Mn.

Table 1. The observed *h k l*, 2θ and *d* values for BTP-Mn crystals.

Unit cell parameters			2θ observed	2θ calculated	*d* (Å) observed
h	*k*	*l*			
1	1	0	12.243	12.242	7.2238
0	0	1	13.434	13.418	6.5857
−1	0	1	16.025	16.026	5.5263
1	0	1	17.671	17.662	5.0150
2	1	1	26.537	26.545	3.3562
0	4	1	30.649	30.673	2.9147
3	1	0	31.613	31.610	2.8279
1	2	2	33.012	32.999	2.7112
−3	2	1	35.347	35.350	2.5373
3	3	0	37.314	37.314	2.4079
−3	1	2	39.891	39.892	2.2581
−4	1	2	48.254	48.271	1.8845

***Step* II**

$$\left[C_2H_5\text{–}P\text{–}(C_6H_5)_3\right]_2[MnBr_4] \xrightarrow{275-360^\circ C} C_4H_{10}\uparrow + 2(C_6H_5)_3PBr\uparrow + Br_2\uparrow + Mn$$

Theoretical loss: 91%
Experimental loss: 90.6%

The decomposition pattern is very clearly seen in the derivative thermogram (DTG) depicted in figure 3 along with TG curves. The exact temperature at which water is

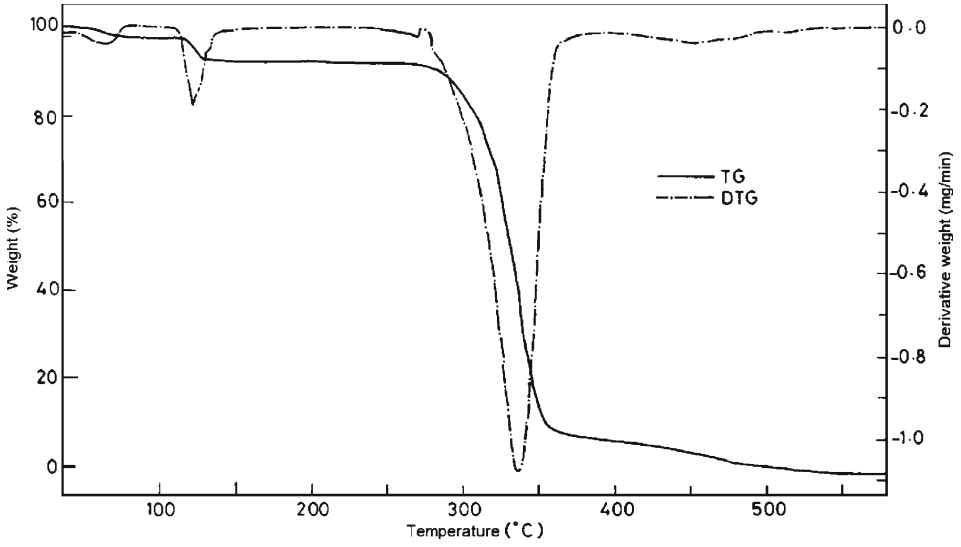

Figure 4. The TG/DTG curves of BTP-Mn.

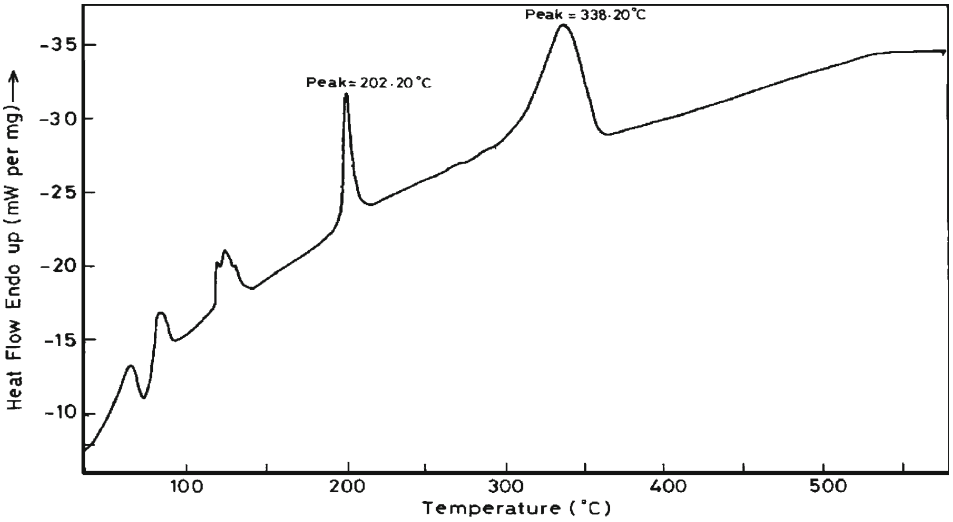

Figure 5. The DTA curve of BTP-Mn.

removed is 121.3°C and the second-step decomposition takes place at 336.7°C as revealed from DTG curves. In DTA shown in figure 5, the peaks at 65 and 75°C are due to the removal of surface water. The peak at 125°C indicates the elimination of two molecules of water of crystallization from the compound. The sharp peak at 202.2°C reflects the melting point of the compound. This is very close to the experimental melting point of the compound (204°C). The broad peak at 338.2°C indicates the large energy requirement of decomposition process.

4.5 *NMR spectral analysis*

The ^{1}H NMR spectrum of BTP-Mn in solution using D_2O as the solvent is shown in figure 6. The ^{1}H NMR spectrum exhibits three proton signals indicating the presence of three different proton environments around 7.6, 3.15 and 1.18 with an intensity ratio of 15 : 2 : 3. The multiplet signal appearing in the aromatic region from δ7.6 to 7.9 ppm is attributed to 15 aromatic protons in the complex species. The broad multiplet signal centred at δ3.7 ppm is due to two methylene protons. The three magnetically equivalent methyl protons appear as broad multiplet centred at δ1.2 ppm.

Figure 7 depicts the ^{13}C NMR spectrum of BTP-Mn. The appearance of distinct carbon signals in the decoupled ^{13}C NMR confirms the molecular structure of the compound. The two carbon signals at δ15.3 and δ15.8 ppm are due to the methylene carbons. The appearance of two different signals for the methylene carbon indicates that they are in slightly different environment. This observation again supports the appearance of broad multiplet for the methylene and methyl protons in the ^{1}H NMR spectrum. The signal at 5.7 ppm is due to the methyl carbon. The carbon signals appearing at δ117, 118, 129, 130, 133 and 134 ppm are due to the aromatic carbon atoms of the three phenyl groups in the complex crystal [16].

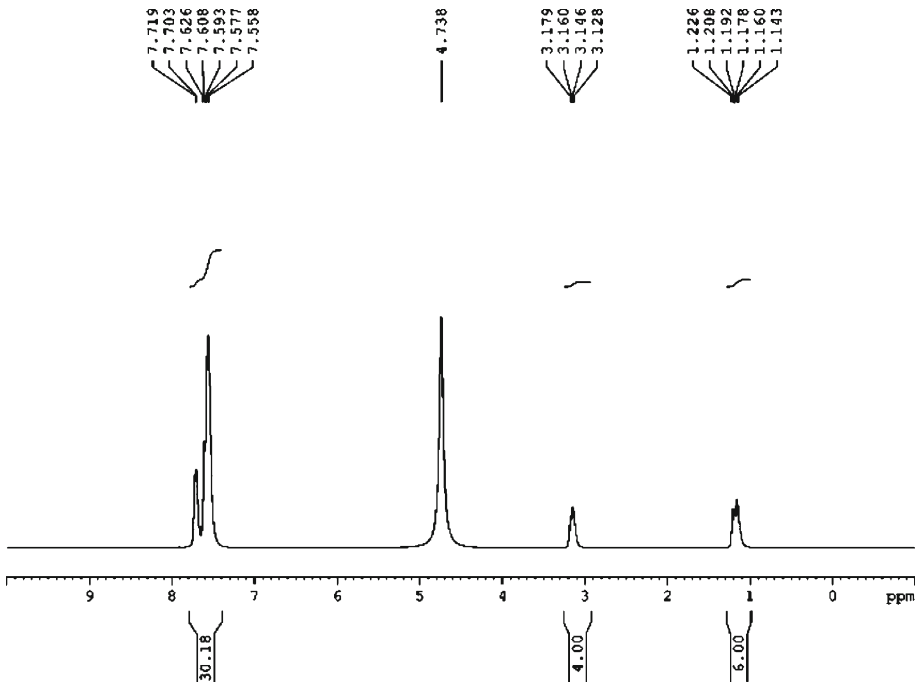

Figure 6. The ^{1}H NMR spectrum of BTP-Mn.

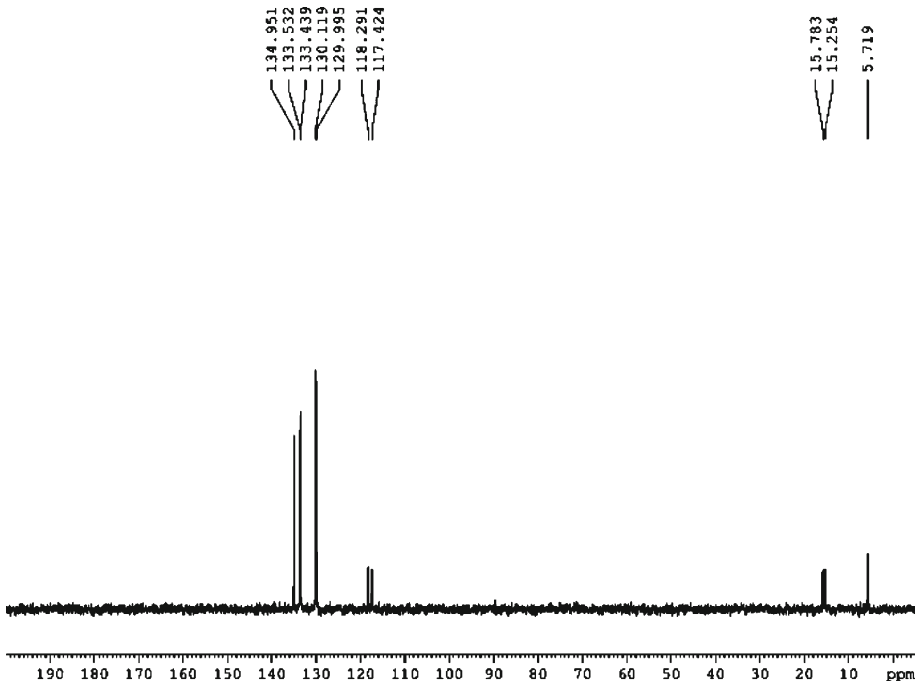

Figure 7. The ^{13}C NMR spectrum of BTP-Mn.

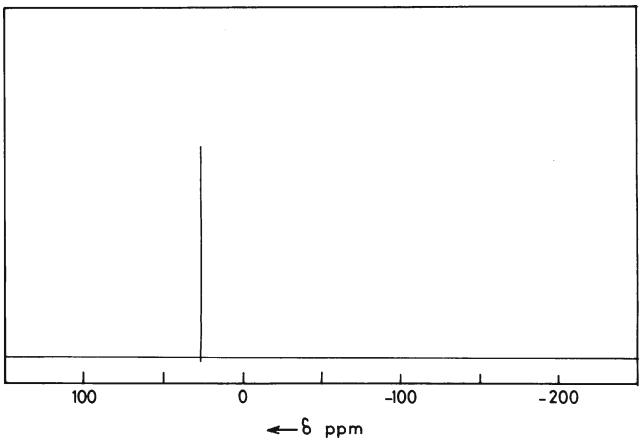

Figure 8. The ^{31}P NMR spectrum of BTP-Mn.

The ^{31}P NMR spectrum is shown in figure 8. The appearance of an intense signal at δ26 ppm accounts for the presence of a phosphorus atom in BTP-Mn.

4.6 *FTIR spectrum*

The FTIR spectrum of BTP-Mn is shown in figure 9 and the absorption frequencies and their assignments are given in table 2. The frequency observed at 3475 cm^{-1} is due to the intermolecular hydrogen bonding as well as asymmetric O–H stretching vibration present

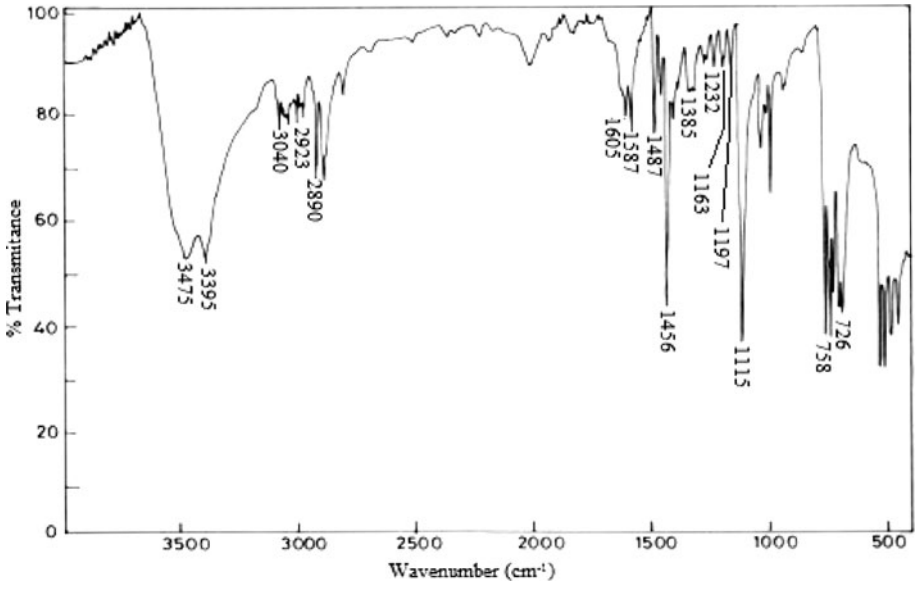

Figure 9. The FTIR spectrum of BTP-Mn.

Table 2. FTIR data of BTP-Mn crystal.

Frequencies (cm^{-1})	Assignments
3475	Intermolecular hydrogen bonding, asymmetric O–H stretching vibration mode
3395	Symmetric O–H stretching vibration mode
3040	Asymmetric C–H stretching of aromatic nucleus
2923	Symmetric C–H stretching of aromatic nucleus, asymmetric C–H stretching vibrations CH_3 and CH_2 groups
2890	Symmetric C–H stretching vibrations of CH_3 and CH_2 groups
1605	C=C stretching (skeletal) of phenyl nucleus
1587	CH_3 asymmetric bending
1487	CH_2 asymmetric bending
1456	CH_3 symmetric bending
1385	CH_2 symmetric bending
1232	C–H in-plane bending of phenyl ring
1163	CH_3 rocking
1197	C–C asymmetric stretching
1115	C–C symmetric stretching
758	CH_2 rocking mode
726	C–C out-of-plane bending in aromatic nucleus

in the compound. The absorption frequency at 3395 cm^{-1} is due to the symmetric O–H stretching vibration mode. The absorption frequency at 3040 cm^{-1} is due to the C–H asymmetric stretching present in the aromatic nucleus. The frequency at 2923 cm^{-1} is due to C–H symmetric stretching present in the aromatic nucleus and asymmetric C–H stretching of CH_3 and CH_2 groups. The frequency at 2890 cm^{-1} is due to the symmetric C–H stretching of CH_3 and CH_2 groups. The absorption frequencies at 1605, 1587, 1487, 1456, 1385 and 1232 cm^{-1} are due to C=C stretching (skeletal) of the phenyl nucleus, CH_3 asymmetric bending, CH_2 asymmetric bending, CH_3 symmetric bending, CH_2 symmetric bending and C–H in-plane bending of the phenyl ring respectively. The absorption frequency at 1163 cm^{-1} is due to CH_3 rocking. The frequencies at 1197, 1115, 758 and 726 cm^{-1} are due to the C–C asymmetric stretching, C–C symmetric stretching, CH_2 rocking mode and C–C out-of-plane bending in the aromatic nucleus of the compound respectively [17].

4.7 *Measurement of second harmonic generation efficiency*

Kurtz SHG test was performed to find the NLO property of BTP-Mn. The sample was illuminated using Spectra-Physics Quanta-Ray DHS-2, Nd:YAG laser using the first harmonic output of 1064 nm with a pulse width of 8 ns. The second harmonic signal, generated in the compound, was confirmed from the emission of green radiation

(532 nm) from the compound. The SHG efficiency of the semiorganic compound is about 1.4 times as large as that of the standard KDP crystal. Beam input energy was 5.7 mJ/pulse.

5. Conclusion

Single crystals of BTP-Mn were grown from saturated solutions by slow evaporation method at room temperature. The grown crystals were characterized by elemental analysis, powder X-ray diffraction, thermal analysis, NMR, FTIR and NLO studies. The elemental analysis of the compound confirmed the stoichiometric ratio. The sharp and well-defined Bragg peaks obtained at specific 2θ angles for the crystals confirmed the crystalline nature of the compound. The decomposition pattern of the compound was formulated based on the TG thermogram and the weight losses observed in the TG curves of the compound fit well with the formulated decomposition pattern. The DTA was also carried out. Various kinds of protons and carbons present in the crystals were confirmed by NMR spectroscopic technique and ^{31}P NMR spectrum confirmed the presence of phosphorous in the compound. The presence of two water molecules and characteristic chemical bonds present in the compounds were confirmed by various absorption frequencies in FTIR spectra. The presence of the nonlinear optical (NLO) property of the grown crystal has been confirmed and this material can be a promising candidate for nonlinear device fabrication.

Acknowledgements

The authors acknowledge the services of Sophisticated Analytical and Instrumentation Facility (SAIF), Indian Institute of Technology, Chennai, Sophisticated Testing and Instrumentation Centre (STIC), Cochin University of Science and Technology, Kochi, School of Chemistry, University of Hyderabad and Indian Institute of Science, Bangalore for their instrumental facilities.

References

[1] Z Tylczynski, P Piskunowicz, A N Nasyrov, A D Karaev, K T Shodiev and G Gulamov, *Phys. Status Solidi* **A133**, 33 (1992)
[2] K Hasebe, H Mashiyama and S Tanisaki, *J. Phys. Soc. Jpn* **49**, 1633 (1980)
[3] H Mayashima and S Tanisaki, *J. Phys. Soc. Jpn* **50**, 1413 (1981)
[4] G Marion, *J. Phys.* **42**, 1469 (1981)
[5] E Fjaer, R A Cowley and T W Ryan, *J. Phys.* **CL41** (1985)
[6] N Hamaya, Y Fujii, S Shimomura, Y Kurowa, S Sasaki and T Matsushita, *Solid State Commun.* **67**, 329 (1988)
[7] N Hamaya, S Shimomura and F Fuji, *J. Phys.: Condens. Matter* **3**, 3387 (1991)
[8] S Shimomura, N Hamaya and Y Fujii, *J. Phys. Soc. Jpn* **65**, 661 (1996)
[9] Y Chen and M B Walker, *Phys. Rev.* **B43**, 5634 (1991)

[10] G Madariaga, F J Zuniga, J M Perez-Mato and M J Tello, *Acta Crystallogr. Sec.* **B43**, 356 (1987)
[11] G Amirthaganesan, M A Kandasamy and M Dhandapani, *Mater. Chem. Phys.* **110**, 328 (2008)
[12] D P Cox, J Terpinski and W Lawrynowicz, *J. Org. Chem.* **49**, 3216 (1984)
[13] D Franzke, C Scherer, O Nuyken and A Wokaun, *J. Photochem. Photobiol.* **AIII**, 47 (1997)
[14] C M Moore, S Hackman, T Brennan and S D Minteer, *J. Membr. Sci.* **254**, 63 (2005)
[15] K Byrappa, M A Kandhaswamy and V Srinivasan, *Cryst. Res. Technol.* **34**, 143 (1999)
[16] W Kemp, *Organic spectroscopy*, 1st edn (The Macmillan Press Ltd, London and Basingstoke, 1975)
[17] R M Silverstein, C G Bassler and T C Morril, in: *Spectroscopic identification of organic compounds*, 5th edn (John Wiley & Sons, New York, 1991) p. 101